Imogolite Nanotubes

Subjects: Nanoscience & Nanotechnology

Contributor: Erwan Paineau

Imogolite nanotubes (INTs) represent a model of nanoplatforms with an untapped potential for advanced technological applications. Easily synthesized by sol-gel methods, these nanotubes are directly obtained with a monodisperse pore size. Coupled with the possibility to adjust their surface properties by using straightforward functionalization processes, INTs form a unique class of diameter-controlled nanotubes with functional interfaces.

imogolite nanotube synthesis functionalization nanocomposite hydrogels molecular sieving liquid crystals catalysis

1. Introduction

Hollow cylinders with a diameter ranging between 1 and 100 nm, so-called nanotubes, are carving out prime positions in nanoscience and nanotechnology. Research into these systems started with Iijima's 1991 seminal article on multi-walled carbon nanotubes (MWCNT) [1]. This was followed by the synthesis in 1993 of single walled carbon nanotubes (SWCNT) of truly nanometric diameters [2][3]. In the meantime, large efforts have been devoted to the study of boron-nitride nanotubes [4] and many different inorganic nanotubes [5][6][7][8][9]. Their physicochemical properties are recognized to be appealing for next-generation devices that could outperform current technologies for nanoelectronics [10], nanofluidics [11], selective molecular sieving [12], energy conversion [13][14], catalytic nanoreactors [15] and carriers for the sustained release of active molecules [16][17][18], to highlight a few. However, most of these applications require controlling at the nanometer scale, the nanotube dimensions (pore size and length), their interface properties as well as their organization, by using straightforward approaches if possible. In this context, having the possibility to synthesize nanotubular structures with desired size and interfaces would be a major step forward in exploring physical concepts in a controlled manner.

Among the wide variety of inorganic nanotubes, imogolite nanotubes (INTs) can boast having these unique and versatile properties. Belonging to clay minerals, these aluminosilicate minerals consist of a curved octahedral [$Al(OH)_3$] layer on which isolated [$SiO_3(OH)$] tetrahedron units are connected upright to the octahedral vacancy via covalent bonding between three mutual oxygen atoms (Figure 1). INT structure can hence be described as a three-dimensional $(OH)_3Al_2O_3Si(OH)$ elementary unit arranged in a hexagonal lattice [19]. It is worth noting that imogolite structure is very different from the one of halloysite, another clay nanotube ubiquitous in soils and weathered rocks, where the curved octahedral [$Al(OH)_3$] layer forms the internal surface of the nanotubes whereas the external surface is composed of Si-O-Si groups [7]. These differences are certainly at the root of the unique properties of imogolite nanotubes.

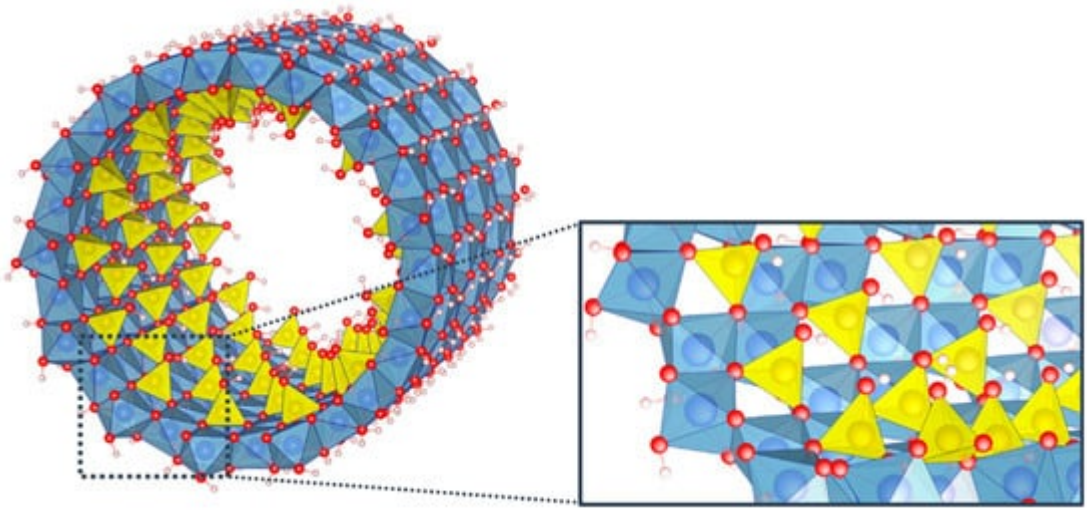

Figure 1. Structure of a single-walled imogolite nanotube and detail of the arrangement of tetrahedron units on the octahedral vacancies. Color code: aluminum (blue); silicon (yellow); oxygen (red); hydrogen (white).

With inner diameters in the nanometer range (1–3 nm), INTs represent one of the most promising inorganic analogs of SWCNTs. Naturally formed from weathered volcanic glass either on Earth [20] or Mars [21], INTs can also be synthesized easily by using low-temperature sol-gel methods [22]. The advantage of INTs originates from a well-defined minimum in the strain energy of the structure [23][24][25][26][27], allowing the production of samples with monodisperse diameter [28][29] and chirality [30], contrarily to other nanotubes where the strain energy decreases monotonically with increasing diameters [31][32]. Coupled with the possibility to adjust either their morphology (single (SW) vs. double-walled (DW) structures, aspect ratio) and surface properties by changing only the nature of the precursors, the synthesis of INT thus offers a convenient and simple way to obtain diameter-controlled nanotubes with functional interfaces. Therefore, they started to be applied in a wide range of potential applications.

2. Imogolite Synthesis

2.1. Synthesis Routes for Aluminosilicate INTs

The synthesis of single-walled imogolite nanotubes (SWINT) was first reported by Farmer et al. in 1977 [22]. It consists of the co-precipitation under vigorous stirring of Al and Si precursors. This solution is adjusted to pH 5 with the addition of NaOH, and then immediately re-acidified to pH 4.5 with a mixture of HCl and acetic acid (Figure 2). Finally, the solution is aged upon heating under reflux or in autoclave. Since then, several improvements have been proposed in the literature by changing either the nature of the precursors, their initial concentration, their ratio (e.g., the hydrolysis ratio R = [OH]/[Al]) or the reaction pathway [33][34][35][36][37][38][39]. Among them, Denaix et al. obtained similar INTs as those reported previously, but without performing the acidification stage [36]. In that case, the hydrolysis step was directly controlled initially by adjusting the amount of NaOH added (typically R = 2, Figure 2). Most of the current studies dealing with INTs use one of the two protocols presented in Figure 2, with minor variations more or less. For instance, the [Al]/[Si] ratio is set between 1.5 and 2, a slight excess of Si precursor preventing the formation of aluminum hydroxides such as gibbsite and boehmite [34]. A “seeding” approach has

also been explored by adding a certain amount of a processed synthetic imogolite sol in a solution of Al and Si precursors [40][41]. Although it avoids the pH adjustment step and allows the imogolite formation after heating the mixture for 2 days, this synthesis route remained quite confidential and has not yet been explored in detail.

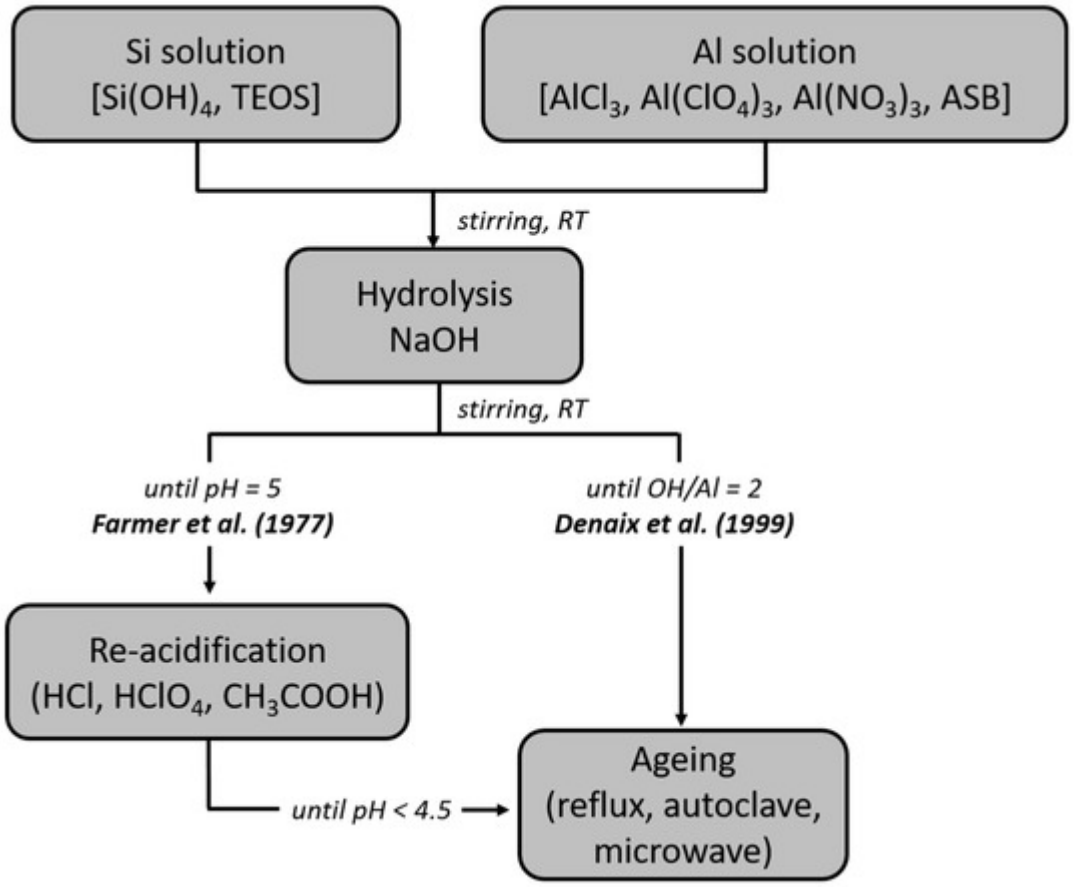

Figure 2. Flowchart for the two main synthesis methods of imogolite nanotubes: Farmer et al. [22]; Denaix et al. [36]. TEOS: tetraethylorthosilicate; ASB: Aluminum tri-sec-butoxide.

2.2. The Selection of Precursors

The sources of Al and Si precursors have also been varied. INT synthesis are commonly performed with $Al(ClO_4)_3$, $AlCl_3$ and Al alkoxide (ASB: aluminum tri-sec-butoxide), $Al(NO_3)_3$ salt being less employed, while the silicon precursor is most often $Si(OH)_4$ or an alkoxide (TEOS: tetraethoxysilane) [38]. However, regardless of the nature of the Al and Si precursors used, the synthetic imogolite nanotubes are always identical with inner and outer diameters of 1 and 2.5 nm, respectively. Conversely, Yucelen et al. suggested that the nature of the protic acid used (HCl, $HClO_4$ or CH_3COOH) may control the relationship between the INT precursor's shape, formed in the early stage of the synthesis (also referred as "proto-imogolite"), and the resulting nanotube shapes [42]. More recently, Arancibia-Miranda et al. evidenced that replacing NaOH with KOH strongly impacts the morphology of the nanotubes in addition to producing a large amount of disordered structures [43]. INT diameter slightly increases by less than 20% while their average length becomes shorter, suggesting that the nature of the counter ions affects the hydrolysis of Al and Si precursors [44][45].

2.3. Effects of Ge Substitution

One of the most blatant examples of progress in INT synthesis arises from the isomorphic substitution of silicon by germanium [46][47]. Beyond a twofold increase in external diameter, replacing TEOS with a Ge alkoxide (e.g., TEOG: tetraethoxygermane) enables producing concentrated (molar) suspensions of Ge-imogolite analogues [48], an important key step towards large scale applications. Maillet et al. observed that the initial concentration of aluminum salt (C_{Al}) controlled the resulting nanotube shape, producing either double-walled (Ge-DWINT, C_{Al} < 0.4 mol·L^{-1}) or single-walled nanotubes (Ge-SWINT, C_{Al} > 0.75 mol·L^{-1}) [49]. The mechanism involved seems to be a subtle balance between attractive and curvature energies during the early stage of the synthesis [49][50]. More interestingly, the energy minimum in the strain energy depends on the substitution ratio [Si]/([Si] + [Ge]) and allows us to predict the INT diameters with respect to the initial synthesis conditions [51][52]. In contrast to Si-INTs, Ge-analogues form short nanotubes with a reduced length (<100 nm) [29][47][52]. On the other hand, Amara et al. demonstrated that micron-long Ge-INTs can be synthesized by using the thermal decomposition of urea ($CO(NH_2)_2$) to produce hydroxyl ions instead of the slow injection of NaOH [53]. Hence, the synthesis of $(OH)_3Al_2O_3Si_xGe_{1-x}(OH)$ INT provides us with a unique system of 1D nanostructures with monodisperse sizes and changeable aspect ratio (Figure 3).

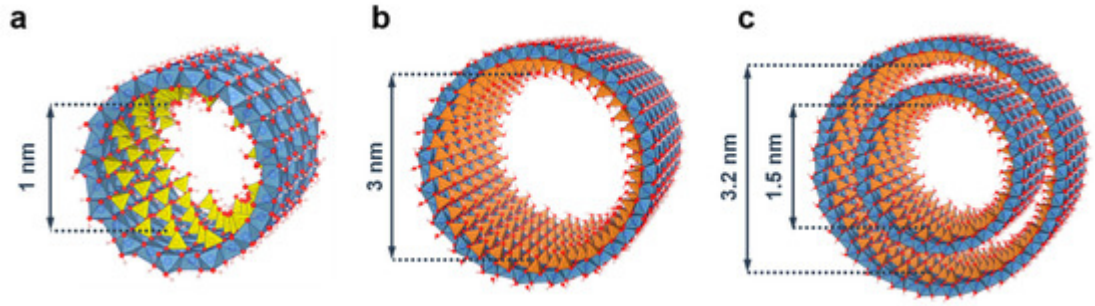

Figure 3. Inner diameter size for the different endmembers of $(OH)_3Al_2O_3Si_xGe_{1-x}(OH)$ imogolite nanotubes. (**a**) Si-SWINT; (**b**) Ge-SWINT; (**c**) Ge-DWINT. Color code: aluminum (blue); silicon (yellow); germanium (orange); oxygen (red); hydrogen (white).

3. Surface Properties and Modifications

3.1. Colloidal Behavior

The structure of INTs with inner and outer hydroxyl groups makes them excellent candidates for colloidal dispersions. Gustafsson moved forward with a unique intrinsic polarization, the isolated –SiOH groups on the inner cavity developing a negative charge, whereas the –AlOHAl groups along the external tube walls bear a weak positive charge [54]. This model has been subsequently corroborated by numerical simulations [24], showing no dependence on the substitution ratio [Si]/([Si] + [Ge]) [25]. Thanks to the surface charge, INTs are easily dispersed in polar solvents to form stable colloidal suspensions [55][56]. Furthermore, the possibility to varying both nanotube aspect ratio (through the synthesis conditions) and electrostatic interactions (pH, ionic strength, …) allows controlling, directly in aqueous phase, the self-organization of imogolite nanotubes from a liquid sol to arrested

phases [57][58][59], making such nanotubes suitable for a wide range of solution processes. Similarly, it is also possible to control the nanotube arrangement in the solid state during the drying process. For instance, powders of Ge-SWINT tend to form large bundles on a 2D hexagonal lattice if they are processed from suspensions prepared at an ionic strength higher than ~10^{-3} mol·L^{-1} [59]. Interestingly, this kind of organization also induces significant radial deformations of the cross section, INTs having a regular hexagonal shape instead of a cylindrical one [60]. Another unique feature of INTs is the high surface density of hydroxyl groups (~18 OH/nm^2), considering the atomic structure reported in [19], which offers multiple binding environments and renders the surface very hydrophilic with high water retention capacity [61][62][63]. INTs were recognized as good adsorbents very early on, especially in environmental contexts where they interact strongly with ions [36][64][65][66][67][68].

Despite these benefits, the presence of water inside INTs might hinder or block the diffusion of other interest molecules (CO_2, CH_4, …). Similarly, in the field of nanocomposites, the effective dispersion of nanoparticles must be achieved only by modifying their surface to make it compatible with the organic matrix. Hence, significant efforts have been undertaken in order to make INTs suitable with the intended applications.

3.2. Modification of the Inner Cavity

Two strategies have been applied for the inner modification of hydrophilic imogolite nanotubes, namely (i) post-synthesis or (ii) direct synthesis chemical procedures. The list of the different coupling agents is summarized in Table 1.

Table 1. Coupling agents used for inner modification (tetrahedral sites) of imogolite nanotubes (INT).

Compound	Acronym	Strategy [a]	INT	Refs.
(3-aminopropyl)triethoxysilane	APTES	post.	Si	[69]
(aminomethyl)triethoxysilane	AMTES	direct	Si	[70]
Methyltrimethoxysilane	MTMS	post.	Si	[71]
		direct	Si	[72]
Methyltriethoxysilane	MTES	direct	Si	[30][72][73][74][75][76]
Trichlorosilane	TCIS	post.	Si	[71]

Compound	Acronym	Strategy [a]	INT	Refs.
Acethyl chloride	AcCl	post.	Si	[71]
Methyltriethoxygermane	MTEG	direct	Ge	[30][75]

[a] Post: post-functionalization; direct: direct synthesis route.

3.3. Modification of the Outer Surface of Imogolite

Modification of the external surface of imogolite has been strongly explored, mainly to render them compatible with another phase. As with the chemical modification of the INT inner cavity, the large density of hydroxyl groups offers a wide range of possibility for surface anchoring and numerous chemical pathways have been proposed with varying degrees of success (Table 2).

Table 2. Main functionalization routes of the outer wall of imogolite nanotube (INT).

Functional Group	Compound	Acronym	INT	Refs.
Silane	(3-aminopropyl)triethoxysilane	APTES	Si	[69][74][77][78]
	(3-chloropropyl)triethoxysilane	CTES	Si	[79]
	(3-mercaptopropyl)trimethoxysilane	MPTMS	Si	[80]
Phosphonate	Octadecylphosphonic acid	ODPA	Si Ge	[81][82][83][84][85] [86]
	Tetradecylphosphonic acid	TDPA	Si	[83]
	Vinylphosphonic acid	VPA	Si	[84]
	Dodecylphosphate	DDPO4	Si	[87]

1. Iijima, S. Helical microtubules of graphitic carbon. Nature 1991, 354, 56–58.
2. Iijima, S.; Ichihashi, T. Single-shell carbon nanotubes of 1-nm diameter. Nature 1993, 363, 603–605.
3. Bethune, D.S.; Klang, C.H.; De Vries, M.S.; Gorman, G.; Savoy, R.; Vazquez, J.; Beyers, R. Cobalt-catalysed growth of carbon nanotubes with single-atomic-layer walls. Nature 1993, 363, 605–607.
4. Chopra, N.G.; Luyken, R.J.; Cherrey, K.; Crespi, V.H.; Cohen, M.L.; Louie, S.G.; Zettl, A. Boron nitride nanotubes. Science 1995, 269, 966–967.

Functional Group	Compound	Acronym	INT	Refs.
Carboxylate	2-Acidphosphoxyethyl methacrylate	P-HEMA	Si	[88]
	Terthiophenes derivatives	HT3P HT3OP	Si	[89]
	8-(2-bromo-2-methylpropanoyloxy)octylphosphate	$BMPOPO_4$	Si	[90]
	Stearic acid	SA	Si	[82]
	Dicarboxylic acid	DA	Si	[91][92]
Sulfonate	Poly[disodium 2,5-bis(3-sulfonatopropoxy)-1,4-phenylene-*alt*-1,4-phenylene)	WS-PPP	Si	[93]
	4-(hydroxyethylthioacetyl)catechol	HETAC	Si	[94]
Others	Benzaldehyde	BA	Si	[95]
	Polypyrrole [a]	ppy	Si	[96][97]
	γ-ray irradiation (peroxides)	-	Si	[98][99]
	Isomorphic substitution (Al → Fe)	Fe-INT	Si Ge	[100][101][102][103][104] [105]

[a] Grafted by chemical vapor deposition (CVD).

26. Lourenco, M.P.; Guimaraes, L.; da Silva, M.C.; de Oliveira, C.; Heine, T.; Duarte, H.A. Nanotubes With Well-Defined Structure: Single- and Double-Walled Imogolites. J. Phys. Chem. C 2014, 118, 5945–5953.

27. Poli, E.; Elliott, J.D.; Hine, N.D.M.; Mostofi, A.A.; Teobaldi, G. Large-scale density functional theory simulation of inorganic nanotubes: A case study on Imogolite nanotubes. Mater. Res.

4. Applications

It is well recognized that imogolite nanotubes remain insulating materials with large band gaps. To tackle this issue, structural modification of the outer wall has also been conducted this time by isomorphic substitution of Al^{3+} by Fe^{3+} [100][101][102][103][104][105]. The effect of Fe incorporation acts as specific coordination centers for organic moieties and leads to higher adsorption efficiency [102][103], while altering the electronic properties of the nanotubes even for low substitution rates [106]. Other isomorphic substitutions have been explored. On the theoretical background, by replacing both Al and Si atoms by elements of groups III (Ga, In) & IV (C, Ge, Sn) respectively [107], or by substituting the inner tetrahedrons by phosphorous and arsenic derivatives [108].

Innov. 2015, 19, S279–S282.

28. Maillet, P.; Levard, C.; Spalla, O.; Masion, A.; Rose, J.; Thill, A. Growth kinetic of single and double-walled aluminogermanate imogolite-like nanotubes: An experimental and modeling approach. Phys. Chem. Chem. Phys. 2011, 13, 2682–2689.

29. Yucelen, G.I.; Kang, D.-Y.; Schmidt-Krey, I.; Beckham, H.W.; Nair, S. A generalized kinetic model for the formation and growth of single-walled metal oxide nanotubes. Chem. Eng. Sci. 2013, 90, 200–212.

30. Monet, G.; Amara, M.S.; Rouzière, S.; Paineau, E.; Chai, Z.; Elliott, J.D.; Poli, E.; Liu, L.-M.; Teobaldi, G.; Launois, P. Structural resolution of inorganic nanotubes with complex stoichiometry. Nat. Commun. 2018, 9, 2033.

31. Hernandez, E.; Goze, C.; Bernier, P.; Rubio, A. Elastic properties of C and BxCyNz composite nanotubes. Phys. Rev. Lett. 1998, 80, 4502.

32. Seifert, G.; Terrones, H.; Terrones, M.; Jungnickel, G.; Frauenheim, T. Structure and electronic properties of MoS2 nanotubes. Phys. Rev. Lett. 2000, 85, 146.

33. Farmer, V.; Adams, M.; Fraser, A.; Palmieri, F. Synthetic Imogolite—Properties, Synthesis, and Possible Applications. Clay Miner. 1983, 18, 459–472.

34. Barrett, S.; Budd, P.; Price, C. The Synthesis and Characterization of Imogolite. Eur. Polym. J. 1991, 27, 609–612.

35. Marzan, L.L.; Philipse, A.P. Synthesis of platinum nanoparticles in aqueous host dispersions of inorganic (imogolite) rods. Colloids Surf. A Physicochem. Eng. Asp. 1994, 90, 95–109.

36. Denaix, L.; Lamy, I.; Bottero, J.Y. Structure and affinity towards Cd2+, Cu2+, Pb2+ of synthetic colloidal amorphous aluminosilicates and their precursors. Colloids Surf. A Physicochem. Eng. Asp. 1999, 158, 315–325.

37. Levard, C.; Masion, A.; Rose, J.; Doelsch, E.; Borschneck, D.; Dominici, C.; Ziarelli, F.; Bottero, J.-Y. Synthesis of Imogolite Fibers from Decimolar Concentration at Low Temperature and Ambient Pressure: A Promising Route for Inexpensive Nanotubes. J. Am. Chem. Soc. 2009, 131, 17080–17081.

38. Chemmi, A.; Brendle, J.; Marichal, C.; Lebeau, B. Key Steps Influencing the Formation of Aluminosilicate Nanotubes by the Fluoride Route. Clays Clay Miner. 2015, 63, 132–143.

39. Lam, C.H.; Yang, A.-C.; Chi, H.-Y.; Chan, K.-Y.; Hsieh, C.-C.; Kang, D.-Y. Microwave-Assisted Synthesis of Highly Monodispersed Single-Walled Alunminosilicate Nanotubes. ChemistrySelect 2016, 1, 6212–6216.

40. Huling, J.C.; Bailey, J.K.; Smith, D.M.; Brinker, C.J. Imogolite as a material for fabrication of inorganic membranes. MRS Online Proc. Libr. Arch. 1992, 271, 511–516.

41. Ackerman, W.; Smith, D.; Huling, J.; Kim, Y.; Bailey, J.; Brinker, C. Gas Vapor Adsorption in Imogolite—A Microporous Tubular Aluminosilicate. Langmuir 1993, 9, 1051–1057.
42. Yucelen, G.I.; Kang, D.-Y.; Guerrero-Ferreira, R.C.; Wright, E.R.; Beckham, H.W.; Nair, S. Shaping Single-Walled Metal Oxide Nanotubes from Precursors of Controlled Curvature. Nano Lett. 2012, 12, 827–832.
43. Arancibia-Miranda, N.; Escudey, M.; Ramirez, R.; Gonzalez, R.I.; van Duin, A.C.T.; Kiwi, M. Advancements in the Synthesis of Building Block Materials: Experimental Evidence and Modeled Interpretations of the Effect of Na and K on Imogolite Synthesis. J. Phys. Chem. C 2017, 121, 12658–12668.
44. Inoue, K.; Huang, P. Influence of Citric-Acid on the Natural Formation of Imogolite. Nature 1984, 308, 58–60.
45. Abidin, Z.; Matsue, N.; Henmi, T. Differential formation of allophane and imogolite: Experimental and molecular orbital study. J. Comput. Aided Mater. Des. 2007, 14, 5–18.
46. Wada, S.; Wada, K. Effects of substitution of germanium for silicon in imogolite. Clays Clay Miner. 1982, 30, 123–128.
47. Mukherjee, S.; Bartlow, V.A.; Nair, S. Phenomenology of the growth of single-walled aluminosilicate and aluminogermanate nanotubes of precise dimensions. Chem. Mater. 2005, 17, 4900–4909.
48. Levard, C.; Rose, J.; Masion, A.; Doelsch, E.; Borschneck, D.; Olivi, L.; Dominici, C.; Grauby, O.; Woicik, J.C.; Bottero, J.-Y. Synthesis of large quantities of single-walled aluminogermanate nanotube. J. Am. Chem. Soc. 2008, 130, 5862–5863.
49. Maillet, P.; Levard, C.; Larquet, E.; Mariet, C.; Spalla, O.; Menguy, N.; Masion, A.; Doelsch, E.; Rose, J.; Thill, A. Evidence of Double-Walled Al-Ge Imogolite-Like Nanotubes. A Cryo-TEM and SAXS Investigation. J. Am. Chem. Soc. 2010, 132, 1208–1209.
50. Thill, A.; Maillet, P.; Guiose, B.; Spalla, O.; Belloni, L.; Chaurand, P.; Auffan, M.; Olivi, L.; Rose, J. Physico-chemical Control over the Single- or Double-Wall Structure of Aluminogermanate Imogolite-like Nanotubes. J. Am. Chem. Soc. 2012, 134, 3780–3786.
51. Konduri, S.; Mukherjee, S.; Nair, S. Controlling nanotube dimensions: Correlation between composition, diameter, and internal energy of single-walled mixed oxide nanotubes. ACS Nano 2007, 1, 393–402.
52. Thill, A.; Guiose, B.; Bacia-Verloop, M.; Geertsen, V.; Belloni, L. How the Diameter and Structure of (OH)(3)Al2O3SixGe1-xOH Imogolite Nanotubes Are Controlled by an Adhesion versus Curvature Cornpetition. J. Phys. Chem. C 2012, 116, 26841–26849.

53. Amara, M.-S.; Paineau, E.; Bacia-Verloop, M.; Krapf, M.-E.M.; Davidson, P.; Belloni, L.; Levard, C.; Rose, J.; Launois, P.; Thill, A. Single-step formation of micron long (OH)3Al2O3Ge(OH) imogolite-like nanotubes. Chem. Commun. 2013, 49, 11284–11286.
54. Gustafsson, J.P. Modelling competitive anion adsorption on oxide minerals and an allophane-containing soil. Eur. J. Soil Sci. 2001, 52, 639–653.
55. Donkai, N.; Inagaki, H.; Kajiwara, K.; Urakawa, H.; Schmidt, M. Dilute-solution properties of imogolite. Makromol. Chem. Macromol. Chem. Phys. 1985, 186, 2623–2638.
56. Karube, J. Hysteresis of the colloidal stability of imogolite. Clays Clay Miner. 1998, 46, 583–585.
57. Philipse, A.P.; Wierenga, A.M. On the density and structure formation in gels and clusters of colloidal rods and fibers. Langmuir 1998, 14, 49–54.
58. Paineau, E.; Krapf, M.-E.M.; Amara, M.-S.; Matskova, N.V.; Dozov, I.; Rouziere, S.; Thill, A.; Launois, P.; Davidson, P. A liquid-crystalline hexagonal columnar phase in highly-dilute suspensions of imogolite nanotubes. Nat. Commun. 2016, 7, 10271.
59. Paineau, E.; Amara, M.S.; Monet, G.; Peyre, V.; Rouzière, S.; Launois, P. Effect of Ionic Strength on the Bundling of Metal Oxide Imogolite Nanotubes. J. Phys. Chem. C 2017, 121, 21740–21749.
60. Amara, M.S.; Rouziere, S.; Paineau, E.; Bacia-Verloop, M.; Thill, A.; Launois, P. Hexagonalization of Aluminogermanate Imogolite Nanotubes Organized into Closed-Packed Bundles. J. Phys. Chem. C 2014, 118, 9299–9306.
61. Karube, J.; Abe, Y. Water retention by colloidal allophane and imogolite with different charges. Clays Clay Miner. 1998, 46, 322–329.
62. Ohashi, F.; Tomura, S.; Akaku, K.; Hayashi, S.; Wada, S.I. Characterization of synthetic imogolite nanotubes as gas storage. J. Mater. Sci. 2004, 39, 1799–1801.
63. Creton, B.; Bougeard, D.; Smirnov, K.S.; Guilment, J.; Poncelet, O. Molecular dynamics study of hydrated imogolite—2. Structure and dynamics of confined water. Phys. Chem. Chem. Phys. 2008, 10, 4879–4888.
64. Clark, C.; McBride, M. Cation and anion retention by natural and synthetic allophane and imogolite. Clays Clay Miner. 1984, 32, 291–299.
65. Clark, C.; McBride, M. Chemisorption of Cu(II) and Co(II) on allophane and imogolite. Clays Clay Miner. 1984, 32, 300–310.
66. Harsh, J.; Traina, S.; Boyle, J.; Yang, Y. Adsorption of cations on imogolite and their effect on surface-charge characteristics. Clays Clay Miner. 1992, 40, 700–706.
67. Arai, Y.; McBeath, M.; Bargar, J.R.; Joye, J.; Davis, J.A. Uranyl adsorption and surface speciation at the imogolite-water interface: Self-consistent spectroscopic and surface complexation models.

Geochim. Cosmochim. Acta 2006, 70, 2492–2509.

68. Levard, C.; Doelsch, E.; Rose, J.; Masion, A.; Basile-Doelsch, I.; Proux, O.; Hazemann, J.-L.; Borschneck, D.; Bottero, J.-Y. Role of natural nanoparticles on the speciation of Ni in andosols of la Reunion. Geochim. Cosmochim. Acta 2009, 73, 4750–4760.
69. Johnson, L.; Pinnavaia, T. Hydrolysis of (gamma-aminopropyl)triethoxysilane-silylated imogolite and formation of a silylated tubular silicate-layered nanocomposite. Langmuir 1991, 7, 2636–2641.
70. Kang, D.-Y.; Brunelli, N.A.; Yucelen, G.I.; Venkatasubramanian, A.; Zang, J.; Leisen, J.; Hesketh, P.J.; Jones, C.W.; Nair, S. Direct synthesis of single-walled aminoaluminosilicate nanotubes with enhanced molecular adsorption selectivity. Nat. Commun. 2014, 5, 3342.
71. Kang, D.-Y.; Zang, J.; Jones, C.W.; Nair, S. Single-Walled Aluminosilicate Nanotubes with Organic-Modified Interiors. J. Phys. Chem. C 2011, 115, 7676–7685.
72. Boyer, M.; Paineau, E.; Bacia-Verloop, M.; Thill, A. Aqueous dispersion state of amphiphilic hybrid aluminosilicate nanotubes. Appl. Clay Sci. 2014, 96, 45–49.
73. Bottero, I.; Bonelli, B.; Ashbrook, S.E.; Wright, P.A.; Zhou, W.; Tagliabue, M.; Armandi, M.; Garrone, E. Synthesis and characterization of hybrid organic/inorganic nanotubes of the imogolite type and their behaviour towards methane adsorption. Phys. Chem. Chem. Phys. 2011, 13, 744–750.
74. Zanzottera, C.; Vicente, A.; Celasco, E.; Fernandez, C.; Garrone, E.; Bonelli, B. Physico-Chemical Properties of Imogolite Nanotubes Functionalized on Both External and Internal Surfaces. J. Phys. Chem. C 2012, 116, 7499–7506.
75. Amara, M.S.; Paineau, E.; Rouziere, S.; Guiose, B.; Krapf, M.-E.M.; Tache, O.; Launois, P.; Thill, A. Hybrid, Tunable-Diameter, Metal Oxide Nanotubes for Trapping of Organic Molecules. Chem. Mater. 2015, 27, 1488–1494.
76. Olson, N.; Deshpande, N.; Gunduz, S.; Ozkan, U.S.; Brunelli, N.A. Utilizing imogolite nanotubes as a tunable catalytic material for the selective isomerization of glucose to fructose. Catal. Today 2018, in press.
77. Johnson, L.; Pinnavaia, T. Silylation of a tubular aluminosilicate polymer (imogolite) by reaction with hydrolyzed (gamma-aminopropyl)triethoxysilane. Langmuir 1990, 6, 307–311.
78. Qi, X.; Yoon, H.; Lee, S.-H.; Yoon, J.; Kim, S.-J. Surface-modified imogolite by 3-APS-OsO4 complex: Synthesis, characterization and its application in the dihydroxylation of olefins. J. Ind. Eng. Chem. 2008, 14, 136–141.
79. Guerra, D.L.; Batista, A.C.; Viana, R.R.; Airoldi, C. Adsorption of rubidium on raw and MTZ- and MBI-imogolite hybrid surfaces: An evidence of the chelate effect. Desalination 2011, 275, 107–

117.

80. Guilment, J.; Martin, D.; Poncelet, O. Hybrid organic-inorganic materials designed to clean wash water in photographic processing: Genesis of a sot-gel industrial product the Kodak Water Saving Treatment System. In Organic/Inorganic Hybrid Materials-2002; Sanchez, C., Laine, R.M., Yang, S., Brinker, C.J., Eds.; Cambridge University Press: Cambridge, UK, 2002; Volume 726, pp. 217–222. ISBN 1-55899-662-1.
81. Yamamoto, K.; Otsuka, H.; Wada, S.; Takahara, A. Surface modification of aluminosilicate nanofiber “imogolite”. Chem. Lett. 2001, 1162–1163.
82. Yamamoto, K.; Otsuka, H.; Takahara, A.; Wada, S.I. Preparation of a novel (polymer/inorganic nanofiber) composite through surface modification of natural aluminosilicate nanofiber. J. Adhes. 2002, 78, 591–602.
83. Park, S.; Lee, Y.; Kim, B.; Lee, J.; Jeong, Y.; Noh, J.; Takahara, A.; Sohn, D. Two-dimensional alignment of imogolite on a solid surface. Chem. Commun. 2007, 28, 2917–2919.
84. Li, M.; Brant, J.A. Dispersing surface-modified imogolite nanotubes in polar and non-polar solvents. J. Nanopart. Res. 2018, 20, 19.
85. Picot, P.; Tache, O.; Malloggi, F.; Coradin, T.; Thill, A. Behaviour of hybrid inside/out Janus nanotubes at an oil/water interface. A route to self-assembled nanofluidics? Faraday Discuss. 2016, 191, 391–406.
86. Bac, B.H.; Song, Y.; Kim, M.H.; Lee, Y.-B.; Kang, I.M. Surface-modified aluminogermanate nanotube by OPA: Synthesis and characterization. Inorg. Chem. Commun. 2009, 12, 1045–1048.
87. Ma, W.; Kim, J.; Otsuka, H.; Takahara, A. Surface Modification of Individual Imogolite Nanotubes with Alkyl Phosphate from an Aqueous Solution. Chem. Lett. 2011, 40, 159–161.
88. Yamamoto, K.; Otsuka, H.; Wada, S.I.; Sohn, D.; Takahara, A. Preparation and properties of [poly(methyl methacrylate)/imogolite] hybrid via surface modification using phosphoric acid ester. Polymer 2005, 46, 12386–12392.
89. Yah, W.O.; Irie, A.; Jiravanichanun, N.; Otsuka, H.; Takahara, A. Molecular Aggregation State and Electrical Properties of Terthiophenes/Imogolite Nanohybrids. Bull. Chem. Soc. Jpn. 2011, 84, 893–902.
90. Ma, W.; Otsuka, H.; Takahara, A. Poly(methyl methacrylate) grafted imogolite nanotubes prepared through surface-initiated ARGET ATRP. Chem. Commun. 2011, 47, 5813–5815.
91. Shikinaka, K.; Kaneda, K.; Mori, S.; Maki, T.; Masunaga, H.; Osada, Y.; Shigehara, K. Direct Evidence for Structural Transition Promoting Shear Thinning in Cylindrical Colloid Assemblies. Small 2014, 10, 1813–1820.

92. Shikinaka, K.; Kikuchi, H.; Maki, T.; Shigehara, K.; Masunaga, H.; Sato, H. Chiral-Linkage-Induced Hierarchical Ordering of Colloidal Achiral Nanotubes in their Thixotropic Gel. Langmuir 2016, 32, 3665–3669.
93. Jiravanichanun, N.; Yamamoto, K.; Irie, A.; Otsuka, H.; Takahara, A. Preparation of hybrid films of aluminosilicate nanofiber and conjugated polymer. Synth. Met. 2009, 159, 885–888.
94. Miura, S.; Teramoto, N.; Shibata, M. Nanocomposites composed of poly(epsilon-caprolactone) and oligocaprolactone-modified imogolite utilizing biomimetic chelating method. J. Polym. Res. 2016, 23, 19.
95. Shikinaka, K.; Abe, A.; Shigehara, K. Nanohybrid film consisted of hydrophobized imogolite and various aliphatic polyesters. Polymer 2015, 68, 279–283.
96. Lee, Y.; Kim, B.; Yi, W.; Takahara, A.; Sohn, D. Conducting properties of polypyrrole coated imogolite. Bull. Korean Chem. Soc. 2006, 27, 1815–1818.
97. Chang, S.; Park, J.; Jang, J.; Lee, J.; Lee, J.; Yi, W. Effect of UV irradiation during synthesis of polypyrrole by a one-step deposition/polymerization process. J. Vacuum Sci. Technol. B 2007, 25, 670–673.
98. Lee, H.; Ryu, J.; Kim, D.; Joo, Y.; Lee, S.U.; Sohn, D. Preparation of an imogolite/poly(acrylic acid) hybrid gel. J. Colloid Interface Sci. 2013, 406, 165–171.
99. Ryu, J.; Kim, H.; Kim, J.; Ko, J.; Sohn, D. Dynamic behavior of hybrid poly (acrylic acid) gel prepared by γ-ray irradiated imogolite. Colloids Surf. A Physicochem. Eng. Asp. 2017, 535, 166–174.
100. Ookawa, M.; Inoue, Y.; Watanabe, M.; Suzuki, M.; Yamaguchi, T. Synthesis and characterization of Fe containing imogolite. Clay Sci. 2006, 12, 280–284.
101. Ookawa, M. Synthesis and Characterization of Fe-Imogolite as an Oxidation Catalyst. Clay Miner. Nat. Their Charact. Modif. Appl. 2013, 239–258.
102. Shafia, E.; Esposito, S.; Manzoli, M.; Chiesa, M.; Tiberto, P.; Barrera, G.; Menard, G.; Allia, P.; Freyria, F.S.; Garrone, E.; et al. Al/Fe isomorphic substitution versus Fe2O3 clusters formation in Fe-doped aluminosilicate nanotubes (imogolite). J. Nanopart. Res. 2015, 17, 336.
103. Shafia, E.; Esposito, S.; Armandi, M.; Manzoli, M.; Garrone, E.; Bonelli, B. Isomorphic substitution of aluminium by iron into single-walled alumino-silicate nanotubes: A physico-chemical insight into the structural and adsorption properties of Fe-doped imogolite. Microporous Mesoporous Mater. 2016, 224, 229–238.
104. Bahadori, E.; Vaiano, V.; Esposito, S.; Armandi, M.; Sannino, D.; Bonelli, B. Photo-activated degradation of tartrazine by H2O2 as catalyzed by both bare and Fe-doped methyl-imogolite nanotubes. Catal. Today 2018, 304, 199–207.

105. Avellan, A.; Levard, C.; Kumar, N.; Rose, J.; Olivi, L.; Thill, A.; Chaurand, P.; Borschneck, D.; Masion, A. Structural incorporation of iron into Ge-imogolite nanotubes: A promising step for innovative nanomaterials. RSC Adv. 2014, 4, 49827–49830.
106. Alvarez-Ramirez, F. First Principles Studies of Fe-Containing Aluminosilicate and Aluminogermanate Nanotubes. J. Chem. Theory Comput. 2009, 5, 3224–3231.
107. Alvarez-Ramirez, F. Theoretical Study of (OH)(3)N2O3MOH, M = C, Si, Ge, Sn and N = Al, Ga, In, with Imogolite-Like Structure. J. Comput. Theor. Nanosci. 2009, 6, 1120–1124.
108. Guimaraes, L.; Pinto, Y.N.; Lourenco, M.P.; Duarte, H.A. Imogolite-like nanotubes: Structure, stability, electronic and mechanical properties of the phosphorous and arsenic derivatives. Phys. Chem. Chem. Phys. 2013, 15, 4303–4309.